

# Honokiol induces autophagic cell death in malignant glioma through reactive oxygen species-mediated regulation of the p53/PI3K/Akt/mTOR signaling pathway



Chien-Ju Lin<sup>a,f</sup>, Ta-Liang Chen<sup>b,g</sup>, Yuan-Yun Tseng<sup>c</sup>, Gong-Jhe Wu<sup>d</sup>, Ming-Hui Hsieh<sup>b,g</sup>, Yung-Wei Lin<sup>e</sup>, Ruei-Ming Chen<sup>a,b,e,f,\*</sup>

<sup>a</sup> Graduate Institute of Medical Sciences, Taipei Medical University, Taipei, Taiwan

<sup>b</sup> Anesthetics and Toxicology Research Center, Taipei Medical University Hospital, Taipei, Taiwan

<sup>c</sup> Department of Neurosurgery, Shuang-Ho Hospital, Taipei Medical University, Taipei, Taiwan

<sup>d</sup> Department of Anesthesiology, Shin Kong Wu Ho-Su Memorial Hospital, Taipei, Taiwan

<sup>e</sup> Brain Disease Research Center, Taipei Medical University Wan-Fang Hospital, Taipei, Taiwan

<sup>f</sup> Comprehensive Cancer Center, Taipei Medical University, Taipei, Taiwan

<sup>g</sup> Department of Anesthesiology, Taipei Medical University Hospital, Taipei, Taiwan

## ARTICLE INFO

### Article history:

Received 9 February 2016

Revised 18 May 2016

Accepted 21 May 2016

Available online 25 May 2016

### Keywords:

Malignant glioma

Honokiol

Autophagy

ROS

p53/PI3K/Akt/mTOR

## ABSTRACT

Honokiol, an active constituent extracted from the bark of *Magnolia officinalis*, possesses anticancer effects. Apoptosis is classified as type I programmed cell death, while autophagy is type II programmed cell death. We previously proved that honokiol induces cell cycle arrest and apoptosis of U87 MG glioma cells. Subsequently in this study, we evaluated the effect of honokiol on autophagy of glioma cells and examined the molecular mechanisms. Administration of honokiol to mice with an intracranial glioma increased expressions of cleaved caspase 3 and light chain 3 (LC3)-II. Exposure of U87 MG cells to honokiol also induced autophagy in concentration- and time-dependent manners. Results from the addition of 3-methyladenine, an autophagy inhibitor, and rapamycin, an autophagy inducer confirmed that honokiol-induced autophagy contributed to cell death. Honokiol decreased protein levels of PI3K, phosphorylated (p)-Akt, and p-mammalian target of rapamycin (mTOR) in vitro and in vivo. Pretreatment with a p53 inhibitor or transfection with p53 small interfering (si)RNA suppressed honokiol-induced autophagy by reversing downregulation of p-Akt and p-mTOR expressions. In addition, honokiol caused generation of reactive oxygen species (ROS), which was suppressed by the antioxidant, vitamin C. Vitamin C also inhibited honokiol-induced autophagic and apoptotic cell death. Concurrently, honokiol-induced alterations in levels of p-p53, p53, p-Akt, and p-mTOR were attenuated following vitamin C administration. Taken together, our data indicated that honokiol induced ROS-mediated autophagic cell death through regulating the p53/PI3K/Akt/mTOR signaling pathway.

© 2016 Elsevier Inc. All rights reserved.

## 1. Introduction

Glioblastoma multiforme (GBM) is the most common and aggressive primary malignant gliomas (Cheng et al., 2012). GBM patients have poor prognoses and high mortality rates due to high mobility and invasion of malignant gliomas (Gunther et al., 2003). The poor outcomes may be because of uncontrolled cell proliferation, infiltrative growth, angiogenesis, and resistance to apoptosis (Staudacher et al., 2014). Honokiol is a bioactive polyphenol extracted from the roots, stem, bark, and seed cones of the Chinese herb *Magnolia officinalis* (Wolf et al., 2007). Honokiol has a variety of pharmacological actions,

such as anti-inflammatory, antithrombotic, antiarrhythmic, neuroprotective, antioxidative, and anxiolytic activities (Xu et al., 2011). Studies also demonstrated that honokiol has antitumor effects by inhibiting proliferation, inducing apoptosis and cell cycle arrest, and suppressing migration and angiogenesis (Hwang and Park, 2010; Chilampalli et al., 2011; Nagalingam et al., 2012). Our previous study demonstrated that honokiol can traverse the blood–brain barrier (BBB), induce apoptosis of neuroblastoma cells via an intrinsic pathway, and induce p53-mediated cell cycle arrest and apoptosis of glioma cells (Lin et al., 2012a). Another study also proved that honokiol induces caspase-independent paraptosis of leukemia cells via reactive oxygen species (ROS) production (Wang et al., 2013). Therefore, the mechanisms of honokiol-induced toxicity of gliomas require further study.

Autophagy is an evolutionarily conserved process for degrading long-lived and misfolded proteins, damaged and dysfunctional

\* Corresponding author at: Graduate Institute of Medical Sciences, College of Medicine, Taipei Medical University, 250 Wu-Xing St., Taipei 110, Taiwan.  
E-mail address: [rmchen@tmu.edu.tw](mailto:rmchen@tmu.edu.tw) (R.-M. Chen).

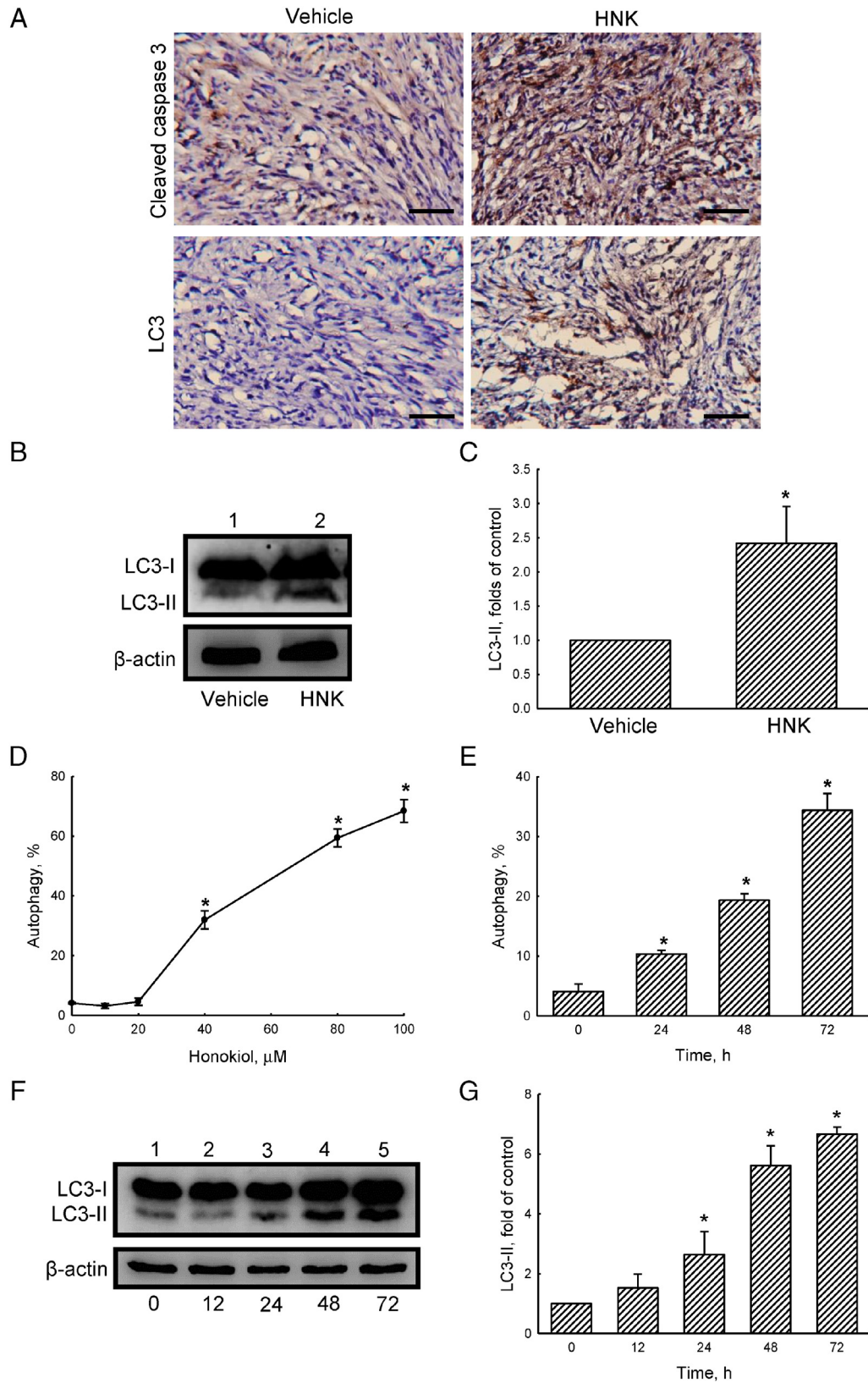


**Fig. 1.** Honokiol (HNK) induces autophagy of glioma cells in vivo and in vitro. Mice with an intracranial glioma and administration of HNK were described in "Materials and methods" (A and B). After being sacrificed, mice brains were removed for immunohistochemical assays of cleaved caspase 3 and light chain 3 (LC3) (A) and immunoblotting analysis of LC3 (B, top panel). Levels of  $\beta$ -actin were analyzed as the internal control (B, bottom panel). LC3-II protein bands were quantified and statistically analyzed (C). Human glioma U87 MG cells were exposed to 10, 20, 40, 80, and 100  $\mu\text{M}$  honokiol for 72 h (D) or to 40  $\mu\text{M}$  honokiol for 24, 48, and 72 h (E). The percentage of cells undergoing autophagy was quantified using flow cytometry with acridine orange staining. U87 MG cells were exposed to 40  $\mu\text{M}$  honokiol for 12, 24, 48, and 72 h (F and G). Levels of LC3 were immunodetected (F, top panel).  $\beta$ -Actin was detected as the internal standard (bottom panel). These protein bands were quantified and statistically analyzed (G). Each value represents the mean  $\pm$  SEM from three independent experiments. \* Values significantly differed from the respective control,  $p < 0.05$ . Scale, 50  $\mu\text{m}$ .

organelles, and foreign particles (Jain et al., 2013). During autophagy, double-membrane vacuoles, called autophagosomes, are formed in the cytoplasm. Microtubule-associated protein light chain 3 (LC3) is essential for the formation of autophagosomes and is important for the

progression of autophagy. Therefore, LC3 is a consistent marker of autophagy (Yoshimori, 2004). Cytoplasmic components embedded in autophagosomes are delivered and degraded in an autolysosome structure (Morselli et al., 2009). Autophagy is critical for the maintenance of

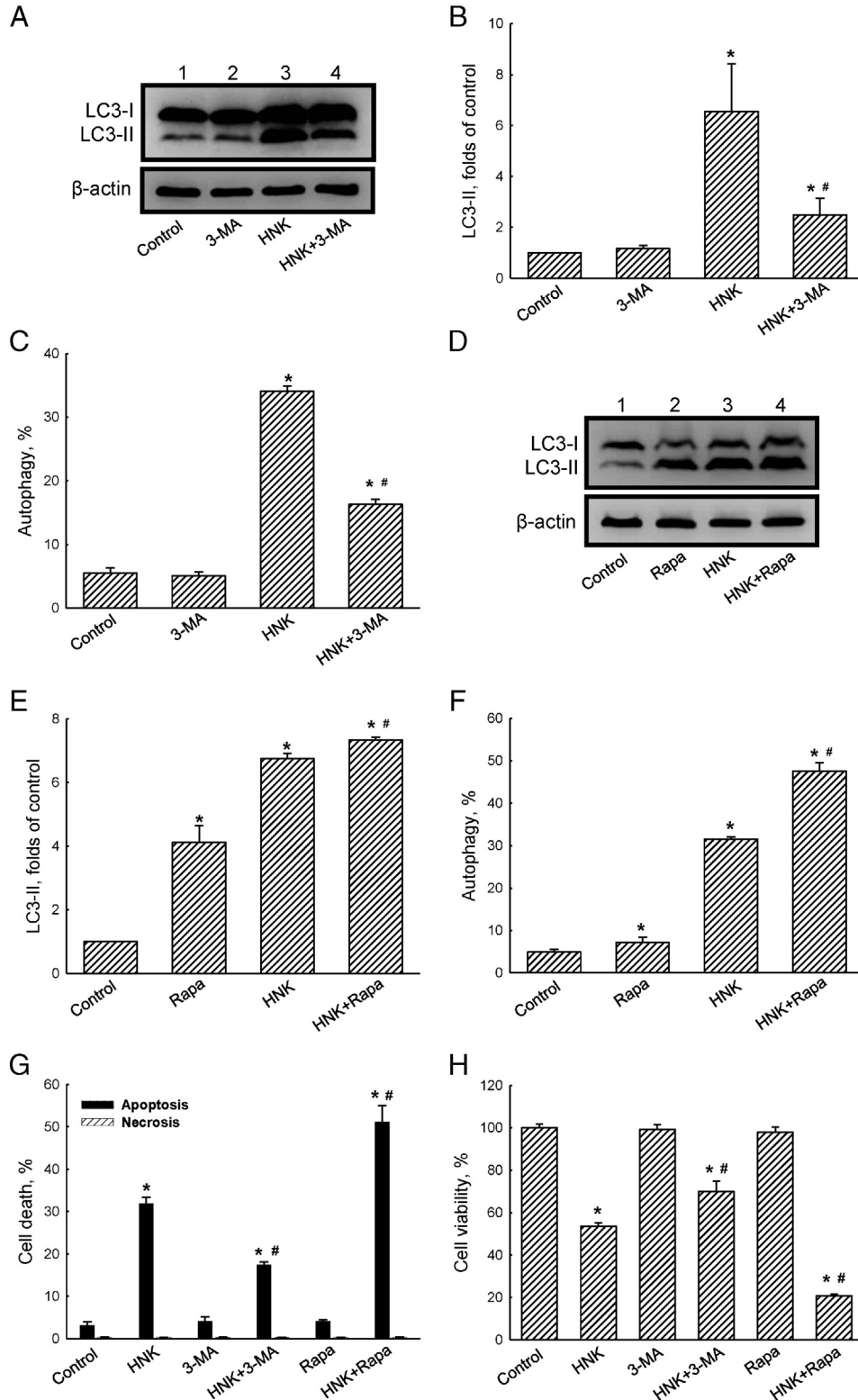


**Fig. 2.** Honokiol (HNK) induces autophagic cell death. Human glioma U87 MG cells were pretreated with 1 mM 3-methyladenine (3-MA) (A–C) or 0.5  $\mu$ M rapamycin (Rapa) (D–F) for 1 h, and then exposed to 40  $\mu$ M HNK for another 72 h. Levels of LC3 were immunodetected (A and D, top panels).  $\beta$ -Actin was detected as the internal control (A and D, bottom panels). These protein bands were quantified and statistically analyzed (B and E). The percentage of autophagy was quantified using flow cytometry with acridine orange staining (C and F). Cell apoptosis was quantified using flow cytometry (G). Cell viability was analyzed using a colorimetric method (H). Each value represents the mean  $\pm$  SEM from three independent experiments. The symbols \* and # indicate that values significantly ( $p < 0.05$ ) differed from the respective control and honokiol-treated groups, respectively.

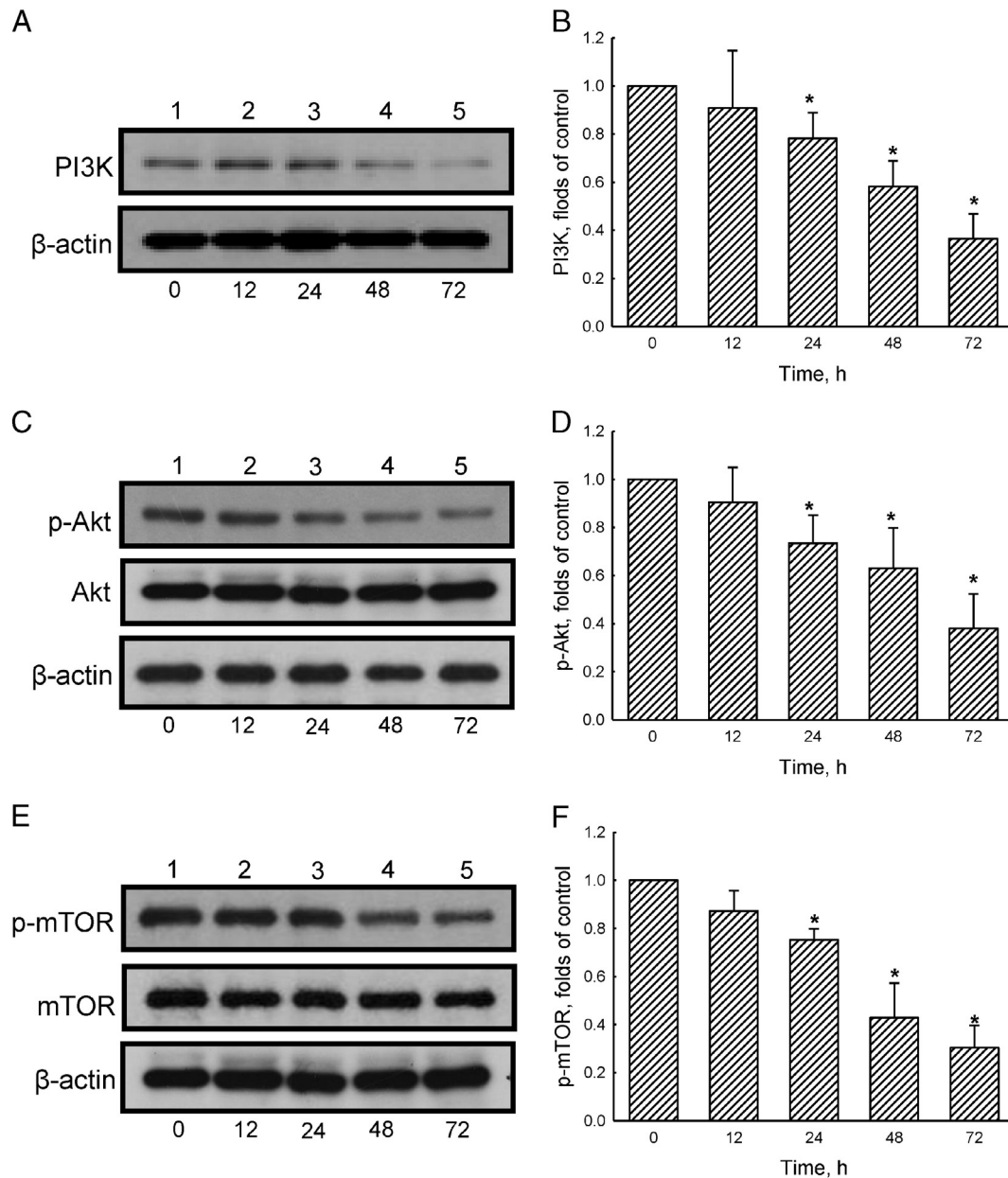


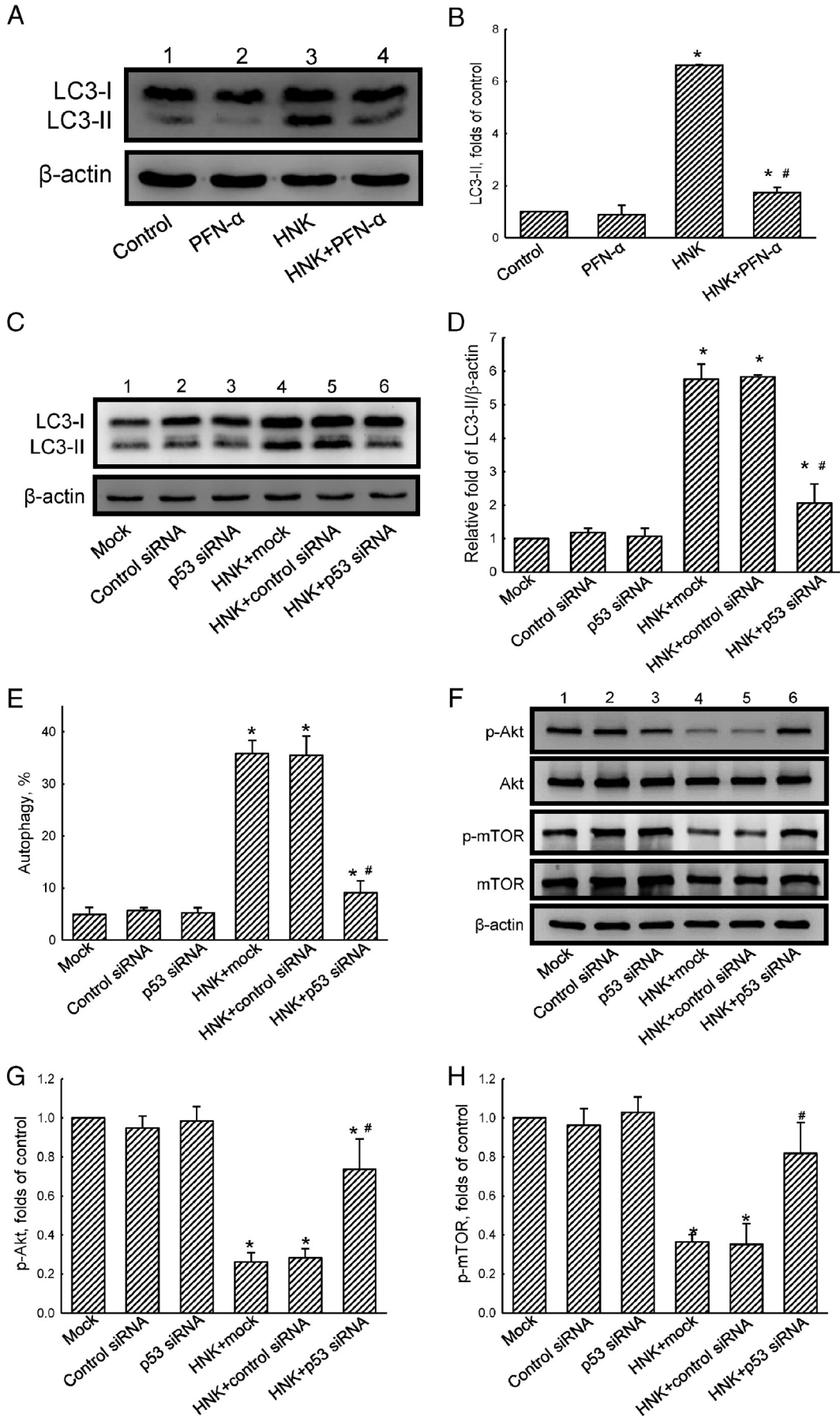
**Fig. 3.** Honokiol (HNK) activates the PI3K/Akt/mammalian target of rapamycin (mTOR) signaling pathway. Human glioma U87 MG cells were exposed to 40  $\mu$ M HNK for 12, 24, 48, and 72 h. Levels of PI3K was immunodetected (A, top panel).  $\beta$ -Actin was detected as an internal control (bottom panel). These protein bands were quantified and statistically analyzed (B). C, Levels of p-Akt and p-mTOR were immunodetected (C and E, top panels). Akt, mTOR, and  $\beta$ -actin were detected as the internal controls (C and E, bottom two panels). These immunorelated protein bands were quantified and statistically analyzed (D and F). Each value represents the mean  $\pm$  SEM from three independent experiments. \* Values significantly differed from the respective control,  $p < 0.05$ .

homeostasis and in certain diseases, such as viral infections, neurodegeneration, cardiovascular diseases, cancers, and aging (Kondo et al., 2010; Mehrpour et al., 2010; Codogno and Mehrpour, 2011).

The mammalian target of rapamycin (mTOR) kinase is important in regulating autophagy as controlled by growth receptors, nutrient depletion, hypoxia, oxidative stress, or low energy (Pattingre et al., 2008). The phosphatidylinositol-3 kinase (PI3K)/Akt signaling pathway activates mTOR through phosphorylating and inactivating the tuberous sclerosis

complex (TSC)1–TSC2 complex, which is inhibited by the LKB1/AMPK signaling pathway (Hay and Sonenberg, 2004; Ding et al., 2011). Inhibition of mTOR results in induction of autophagy (Jones, 2009). Activation of p53, a tumor suppressor protein which regulates cell survival under genomic stress by inducing cell cycle arrest and apoptosis, also stimulates autophagy through inhibiting the mTOR pathway (Vousden and Lu, 2002; Jones, 2009; Zhuang et al., 2009). Anticancer agents, such as curcumin and naringin, can induce autophagy-mediated growth

**Fig. 4.** p53 contributes to honokiol (HNK)-induced autophagy. Human glioma U87 MG cells were pretreated with 10  $\mu$ M PFN- $\alpha$ , an inhibitor of p53, for 1 h, and then exposed to 40  $\mu$ M HNK for another 72 h. The level of LC3 was immunodetected (A, top panel).  $\beta$ -Actin was detected as the internal standard (bottom panel). LC3-II protein bands were quantified and statistically analyzed (B). U87 MG cells were transfected with 80 nM of the negative control or p53 siRNA for 24 h and then treated with 40  $\mu$ M HNK for another 72 h. Levels of LC3 and  $\beta$ -actin were immunodetected (C), and these protein bands were quantified and statistically analyzed (D). The percentage of cells undergoing autophagy was quantified using flow cytometry (E). Levels of p-Akt and p-mammalian target of rapamycin (mTOR) were immunodetected (F, first and third panels). Akt, mTOR, and  $\beta$ -actin were detected as the internal controls (F, second, fourth, and bottom panels). These protein bands were quantified and statistically analyzed (G and H). Each value represents the mean  $\pm$  SEM from three independent experiments. The symbols \* and # indicate that values significantly ( $p < 0.05$ ) differed from the respective control and honokiol-treated groups, respectively.



inhibition of tumor cells (Aoki et al., 2007; Raha et al., 2015). However, determining whether honokiol induces autophagy in glioma cells requires further study. Thus, in this study, we investigated the effect and mechanism of honokiol-induced autophagy of glioma cells.

## 2. Materials and methods

### 2.1. Animal orthotopic brain tumor model and drug treatment

All procedures were performed according to the *Guide for the Care and Use of the Laboratory Animals* published by the US National Institutes of Health (NIH Publication no. 85-23, revised 1996) and approved by the Institutional Animal Care and Use Committee of Taipei Medical University (Taipei, Taiwan). Six-week-old female nude mice (BALB/c nu/nu) purchased from the National Laboratory Animal Center, Taipei, Taiwan were housed in a sterile environment (in a specific pathogen-free room) with a 12/12-h light/dark cycle and were allowed free access to food and water for 1 week. An intracranial glioma model was created as described previously (Lin et al., 2016). Briefly, animals were anesthetized by inhalation of isoflurane and then were stereotactically inoculated with  $2 \times 10^5$  U87 MG cells (in 3  $\mu$ l phosphate-buffered saline; PBS) in the right frontal lobe (2 mm lateral and 1 mm anterior to the bregma, at 3 mm in depth from the skull base) using a Hamilton syringe (Reno, NV) and a syringe pump (SINGA Technology, Taipei, Taiwan). Intracranial glioma-bearing mice were randomly divided into two groups ( $n = 3/\text{group}$ ) 4 days after tumor implantation and were intraperitoneally injected with 20 mg/kg honokiol or vehicle (10% dimethyl sulfoxide (DMSO) in PBS) two times per week for 2 weeks. Mice were sacrificed 3 weeks after implantation of glioma cells. Brains were removed for further analyses. Gliomas were measured according to body weight loss, a Kaplan–Meier survival analysis, and immunohistochemical analyses of epidermal growth factor receptor and caspase-3 as described previously (Lin et al., 2016).

### 2.2. Histology and immunohistochemistry

Brain tissues were fixed in 4% paraformaldehyde in PBS, embedded in paraffin, and sectioned. Sections were deparaffinized with xylene, rehydrated with a graded alcohol series, followed by antigen target retrieval for 20 min. Endogenous peroxidase activity was quenched in a 3% H<sub>2</sub>O<sub>2</sub> solution. Slides were incubated in blocking solution (Vector Laboratories, Burlingame, CA) for 1 h. Primary antibodies for cleaved caspase 3 and LC3 (1:300, Cell Signaling, Beverly, MA) were incubated at 4 °C overnight followed by incubation with biotin-conjugated secondary antibodies, for 1 h at room temperature. Slides were subsequently detected using a Vectastain ABC kit (Vector Laboratories). 3,3'-Diaminobenzidine (DAB, Vector Laboratories) is a substrate for peroxidase. Sections were counterstained with hematoxylin, followed by dehydration in a graded alcohol series and xylene, with the addition of a coverslip. Photomicrographs were taken at 200 $\times$  magnification with a Nikon microscope equipped with a digital camera (Nikon, Melville, NY).

### 2.3. Cell culture and drug treatment

The human glioma U87 MG cell line was purchased from the American Type Culture Collection (Manassas, VA). Cells were maintained in minimum essential medium (Gibco-BRL Life Technologies, Grand Island, NY) supplemented with 10% fetal bovine serum, 2 mM L-

glutamine, 100 IU/ml penicillin, 100 mg/ml streptomycin, 1 mM sodium pyruvate, and 1 mM nonessential amino acids at 37 °C in a humidified atmosphere of 5% CO<sub>2</sub>. Cells were grown to confluence before drug treatment. Honokiol was purchased from Sigma (St. Louis, MO) and was freshly dissolved in DMSO. Cells were exposed to different concentrations of honokiol and/or other agents indicated in the text for various intervals.

### 2.4. Detection of acidic vesicular organelles (AVOs)

Flow cytometry with acridine orange staining as described in a previous study was used to detect and quantify the AVOs, one of the characteristics of autophagy (Kanzawa et al., 2003). At the end of individual experiments, U87 MG cells were collected in phenol red-free RPMI 1640 medium. Green (FL-1) and red (FL-3) fluorescences of acridine orange were measured using a flow cytometer and CellQuest software (Becton Dickinson, San Jose, CA). The sum of the upper-left and upper-right quadrants of the cytogram was used to estimate the percentage of cells undergoing autophagy.

### 2.5. Quantification of apoptotic and necrotic cells

The mode of cell death was analyzed by flow cytometry with annexin V/propidium iodide (PI) double-staining to detect membrane events according to a previous study (Lin et al., 2012a, 2012b). After individual treatments, whole cells were collected in 4-(2-hydroxyethyl)-1-piperazineethanesulfonic acid (HEPES) buffer containing 10 mM HEPES (pH 7.4), 140 mM NaCl, and 2.5 mM CaCl<sub>2</sub>. Cells were subsequently stained with annexin V (2.5  $\mu$ g/ml) and PI (2 ng/ml) for 20 min, followed by analysis by flow cytometry (Beckman Coulter). Cytograms of the four quadrants in the figure were used to distinguish normal (annexin V<sup>-</sup>/PI<sup>-</sup>), early apoptotic (annexin V<sup>+</sup>/PI<sup>-</sup>), late apoptotic (annexin V<sup>+</sup>/PI<sup>+</sup>), and necrotic cells (annexin V<sup>-</sup>/PI<sup>+</sup>). The sum of early apoptosis and late apoptosis is presented as total apoptosis.

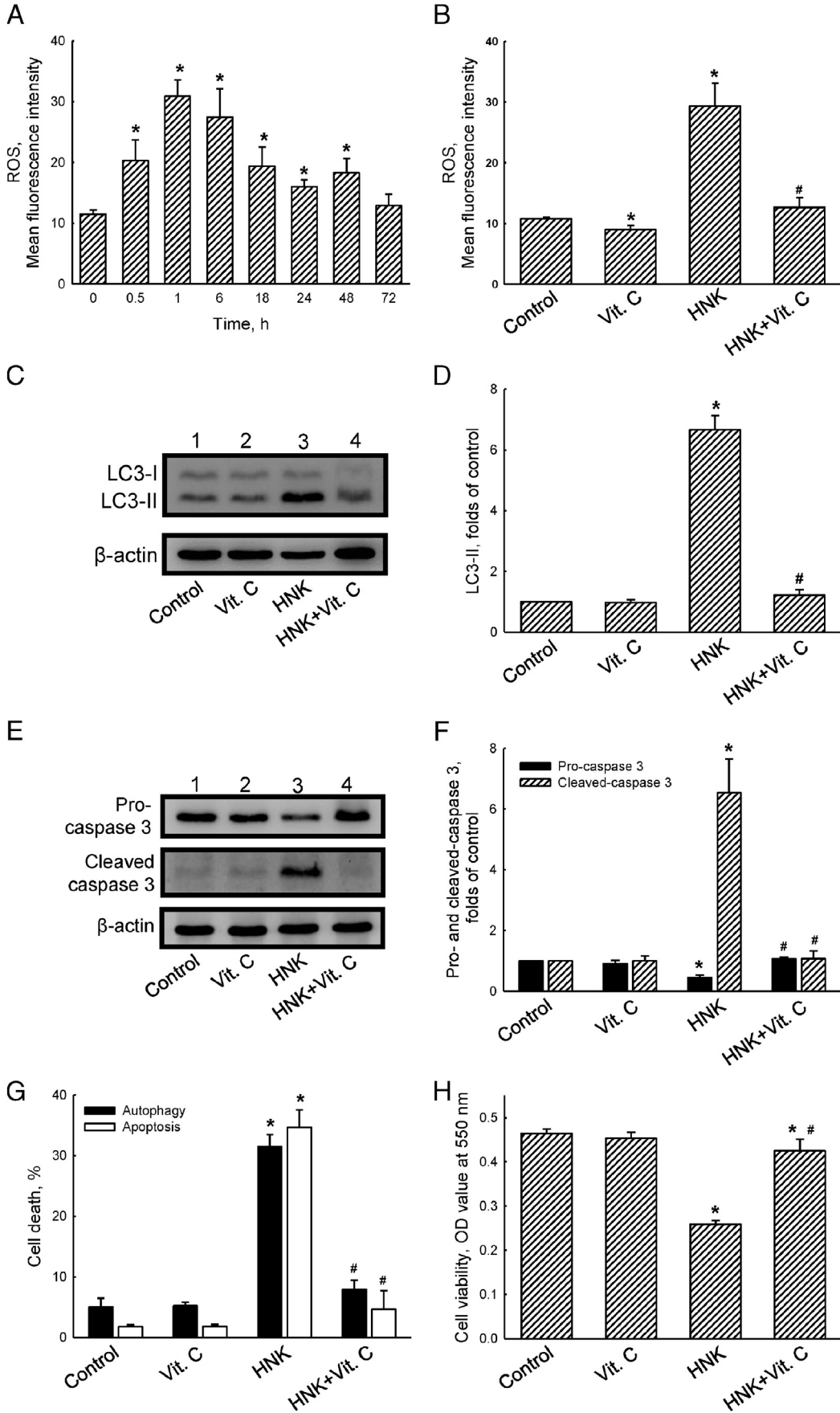
### 2.6. Cell viability assay

Cell viability was assayed using 3-(4,5-dimethylthiazol-2-yl)-2,5-diphenyltetrazolium bromide (MTT). U87 MG cells were seeded on a 96-well plate at  $8 \times 10^3$  cells/well for 24 h, followed by drug treatment for another 72 h. Before the end of treatment, 0.5 mg/ml MTT was added to each well for 4 h. Supernatants were carefully aspirated, and formazan crystals were dissolved in DMSO. Absorbance was measured at 550 nm with an Anthos 2020 Microplate Reader (Biochom, Holliston, MA).

### 2.7. Immunoblotting

After drug treatment, U87 MG cells or tumor tissues were lysed with ice-cold lysis buffer (25 mM HEPES, 1.5% Triton X-100, 0.1% sodium dodecylsulfate (SDS), 0.5 M NaCl, 5 mM EDTA, and 0.1 mM sodium deoxycholate) containing a protease inhibitor cocktail. Protein concentrations were quantified using a bicinchoninic acid protein assay kit (Thermo, San Jose, CA). An equal amount of protein from each group was separated using SDS-polyacrylamide gel electrophoresis (PAGE), followed by transfer to nitrocellulose membranes. Membranes were incubated with a 5% skim milk solution (blocking solution) for 1 h, and then incubated with indicated antibodies at 4 °C for 16 h. Membranes were probed with the appropriate horseradish peroxidase-conjugated

**Fig. 5.** Reactive oxygen species (ROS) are involved in honokiol (HNK)-induced autophagic death. Human glioma U87 MG cells were treated with 40  $\mu$ M HNK for 0–72 h. Levels of intracellular ROS were analyzed by flow cytometry (A). U87 MG cells were pretreated with 250  $\mu$ M vitamin C (Vit. C) for 1 h and then with 40  $\mu$ M HNK for another 6 h, and amounts of intracellular ROS were analyzed (B). Levels of LC3 and pro- and cleaved caspase-3 were immunodetected (C and E, top panels).  $\beta$ -Actin was immunodetected as the internal control (C and E, bottom panels). These protein bands were quantified and statistically analyzed (D and F). Cell apoptosis (G) and cell viability were analyzed using flow cytometry and a colorimetric method. Each value represents the mean  $\pm$  SEM from three independent experiments. The symbols \* and # indicate that values significantly ( $p < 0.05$ ) differed from the respective control and honokiol-treated groups, respectively.



secondary antibodies for 1 h at room temperature. Immunoreactive proteins were detected using an enhanced chemiluminescence reagent (Western Lightning™ Plus-ECL, PerkinElmer, Waltham, MA) and then imaged using a Syngene G:BOX iChemi camera (Syngene, Cambridge, UK) and GeneSnap software (vers. 7.09, Syngene). Anti-LC3, PI3K, p-Akt, Akt, p-mTOR, mTOR, p-p53, and caspase 3 antibodies were purchased from Cell Signaling Technology (Beverly, MA). Anti-p53 and p62 antibodies were purchased from Santa Cruz Biotechnology (Santa Cruz, CA). An anti- $\beta$ -actin antibody was purchased from Sigma (St. Louis, MO). The density of bands was determined with Gel-Pro Analyzer densitometry software.

### 2.8. Knockdown of p53

The p53 small interfering (si)RNA and control siRNA were obtained from Santa Cruz Biotechnology. U87 MG cells were transfected with siRNA using the lipofectamine RNAimax reagent (Invitrogen, San Diego, CA) according to the manufacturer's instructions. In brief, cells were incubated with the lipofectamine RNAimax reagent and 80 nM of siRNA for 6 h; the medium was subsequently refreshed, followed by incubation for 24 h. Transfected cells were treated with honokiol for another 72 h and analyzed by the indicated experiments.

### 2.9. Measurement of ROS production

Levels of intracellular ROS were detected using the probe 2,7-dihydrodichlorofluorescein diacetate. U87 MG cells were collected after the indicated treatments. After trypsinization, cells were resuspended in PBS and stained with 10  $\mu$ M DCFH-DA for 30 min at 37 °C in the dark. The fluorescence was measured on a flow cytometer (Beckman Coulter, Brea, CA). The mean fluorescence intensity was calculated by CellQuest software and represents the level of ROS production.

### 2.10. Statistical analysis

The statistical significance of differences between the control and drug-treated groups was evaluated using Student's *t*-test; differences between drug-treated groups were evaluated using Duncan's multiple-range test. Statistical analyses between groups over time were carried out by a two-way analysis of variance. A *p* value of <0.05 was considered statistically significant.

## 3. Results

After administration of honokiol to mice bearing an intracranial glioma, honokiol increased expressions of cleaved caspase 3 and LC3 in tumor tissues (Fig. 1A). The protein level of LC3 purified from tumor tissues was analyzed by immunoblotting (Fig. 1B). After the mice were administered honokiol, levels of LC3 increased by 2.5-fold (Fig. 1C). The *in vitro* effect of honokiol on inducing autophagy was also evaluated. Treatment of U87 MG cells with 10 and 20  $\mu$ M honokiol for 72 h did not induce autophagy (Fig. 1D). When the administered concentrations reached 40, 80, and 100  $\mu$ M, honokiol caused significant 32.0%, 59.4%, and 68.4% of cells to undergo autophagy, respectively. In the time course experiment, after U87 MG cells were treated with 40  $\mu$ M honokiol for 24, 48, and 72 h, percentages of cells undergoing autophagy had increased to 10.4%, 19.3%, and 34.4%, respectively (Fig. 1E). In addition, the LC3-II protein in honokiol-treated U87 MG cells increased (Fig. 1F, top panel, lanes 3 to 5). When treated with honokiol for 24, 48, and 72 h, levels of LC3-II increased 2.6-, 5.6-, and 6.7-fold, respectively (Fig. 1G). After treatment with honokiol for 24, 48, and 72 h, levels of p62 and beclin-1, autophagy-related proteins, were altered (see Figs. 1A and 2 in Wu et al., 2016).

The role of honokiol-induced autophagy in cell death was further analyzed (Fig. 2). When U87 MG cells were pretreated with the autophagy

inhibitor, 3-methyladenine (3-MA), the honokiol-induced increase in LC3-II was suppressed (Fig. 2A, top panel, lane 4). Compared to the honokiol alone group, exposure of U87 MG cells to 1 mM 3-MA and 40  $\mu$ M honokiol decreased the level of LC3-II from 6.6- to 2.5-fold (Fig. 2B). Combined treatment with 3-MA and honokiol for 72 h caused a 17.8% decrease in cells undergoing autophagy (Fig. 2C). In contrast, when U87 MG cells were only treated with 0.5  $\mu$ M rapamycin, an autophagy inducer, or when cells were pretreated for 1 h followed by 40  $\mu$ M honokiol for another 24 h, levels of LC3-II increased (Fig. 2D, top panel, lanes 2 and 4). Rapamycin alone and combined with honokiol respectively increased the level of LC3-II to 4.1- and 7.3-fold (Fig. 2E). Rapamycin also increased honokiol-induced autophagy from 31.5% to 47.6% (Fig. 2F). After U87 MG cells were pretreated with 1 mM 3-MA for 1 h and then 40  $\mu$ M honokiol for another 72 h, the percentage of honokiol-induced apoptosis decreased from 31.9% to 17.5% (Fig. 2G), whereas pretreatment with rapamycin increased the percentage of apoptosis to 51.2% (Fig. 2G). Subsequently, combining 3-MA and honokiol resulted in an increase in cell viability, but rapamycin further suppressed cell viability (Fig. 2H).

Treatment of human U87 MG glioma cells with 40  $\mu$ M honokiol for 12–72 h suppressed the protein level of PI3K (Fig. 3A, top panel). When treated with honokiol for 12, 24, 48, and 72 h, levels of PI3K decreased to 0.91-, 0.78-, 0.58-, and 0.37-fold, respectively (Fig. 3B). The level of p-Akt also decreased due to honokiol (Fig. 3C, top panel). After exposure of human U87 MG glioma cells to 40  $\mu$ M honokiol for 24, 48, and 72 h, levels of the p-Akt protein significantly decreased to 0.73-, 0.63-, and 0.38-fold, respectively (Fig. 3D). Meanwhile, amounts of p-mTOR were also suppressed by honokiol (Fig. 3E, top panel). Exposure of human U87 MG glioma cells to 40  $\mu$ M honokiol for 24, 48, and 72 h respectively decreased the level of p-mTOR to 0.75-, 0.43-, and 0.30-fold (Fig. 3F). Administration of honokiol decreased levels of p-Akt and p-mTOR (see Fig. 3 in Wu et al., 2016).

The role of p53 in honokiol-induced autophagy was investigated in this study (Fig. 4). Pretreatment of U87 MG cells with the p53 inhibitor, pifithrin- $\alpha$ , p-nitro, cyclic (PFN- $\alpha$ ), blocked honokiol-induced LC3 processing to LC3-II (Fig. 4A, top panel). After U87 MG cells were pretreated with 10  $\mu$ M PFN- $\alpha$  and then 40  $\mu$ M honokiol for another 72 h, the level of LC3-II decreased from 6.6- to 1.7-fold (Fig. 4B). Furthermore, pretreatment of U87 MG cells with p53 siRNA for 24 h caused a significant 86% reduction in levels of p53 (data not shown). Knockdown of p53 decreased the level of LC3-II (Fig. 4C, top panel). After U87 MG cells were transfected with 80 nM p53 siRNA for 24 h followed by treatment with honokiol for another 72 h, the level of LC3-II decreased from 5.8- to 2.1-fold (Fig. 4D). In addition, transfection of p53 siRNA reduced the percentage of honokiol-induced autophagy from 35.9% to 9.1% (Fig. 4E). In parallel, levels of p-Akt and p-mTOR were also reversed due to knockdown of p53 (Fig. 4F, top and third panels). Transfection of 80 nM p53 siRNA into human U87 MG glioma cells for 24 h followed by 40  $\mu$ M honokiol for 72 h increased the level of p-Akt from 0.26- to 0.74-fold (Fig. 4G). Similarly, the level of p-mTOR increased from 0.36- to 0.82-fold (Fig. 4H).

To investigate the role of ROS in honokiol-induced cell death, the level of intracellular H<sub>2</sub>O<sub>2</sub> was measured. After exposure of U87 MG cells to 40  $\mu$ M honokiol, the level of H<sub>2</sub>O<sub>2</sub> significantly increased to 1.8-fold within 0.5 h, had reached a maximum of 2.7-fold at 1 h, and then this was sustained to 48 h (Fig. 5A). After U87 MG cells were pretreated with 250  $\mu$ M vitamin C, an antioxidant, for 1 h and then 40  $\mu$ M honokiol for another 6 h, the level of honokiol-induced ROS decreased from 2.7- to 1.2-fold (Fig. 5B). The level of the LC3-II protein was also reduced by vitamin C (Fig. 5C, top panel, lane 4). Exposure of U87 MG cells to vitamin C and honokiol reduced levels of LC3-II from 6.7- to 1.2-fold (Fig. 5D). In parallel, the honokiol-induced cleavage of caspase 3 was suppressed by vitamin C (Fig. 5E, second panel, lane 4). After treatment with vitamin C and honokiol for 72 h, the level of procaspase 3 was reversed, whereas the level of cleaved caspase 3 was reduced (Fig. 5F). Consequently, pretreatment with vitamin C decreased

the percentage of autophagy from 31.5% to 7.9%, and the percentage of apoptosis from 34.7% to 4.7% (Fig. 5G). Therefore, the viability of U87 MG cells increased when 40  $\mu$ M honokiol and vitamin C were used in combination (Fig. 5H).

To further investigate the relationship between ROS and honokiol-induced autophagy, expressions of proteins were subjected to immunoblotting (Fig. 6). The increased protein levels of p-p53 and p53 were reduced by the addition of vitamin C (Fig. 6A, top two panels, lane 4).

Exposure of U87 MG cells to vitamin C and honokiol for 72 h reduced levels of p-p53 from 2.9- to 1.2-fold (Fig. 6B, black columns), and levels of p53 from 1.9- to 1.1-fold (Fig. 6B, gray columns). Meanwhile, the level of p-Akt was reversed by vitamin C (Fig. 6C, top panel, lane 4). After treatment with 250  $\mu$ M vitamin C and 40  $\mu$ M honokiol for 72 h, the level of p-Akt increased from 0.48- to 0.91-fold (Fig. 6D). Similarly, the addition of vitamin C increased the p-mTOR level (Fig. 6E). The level of p-mTOR increased from 0.47- to 0.92-fold (Fig. 6F).

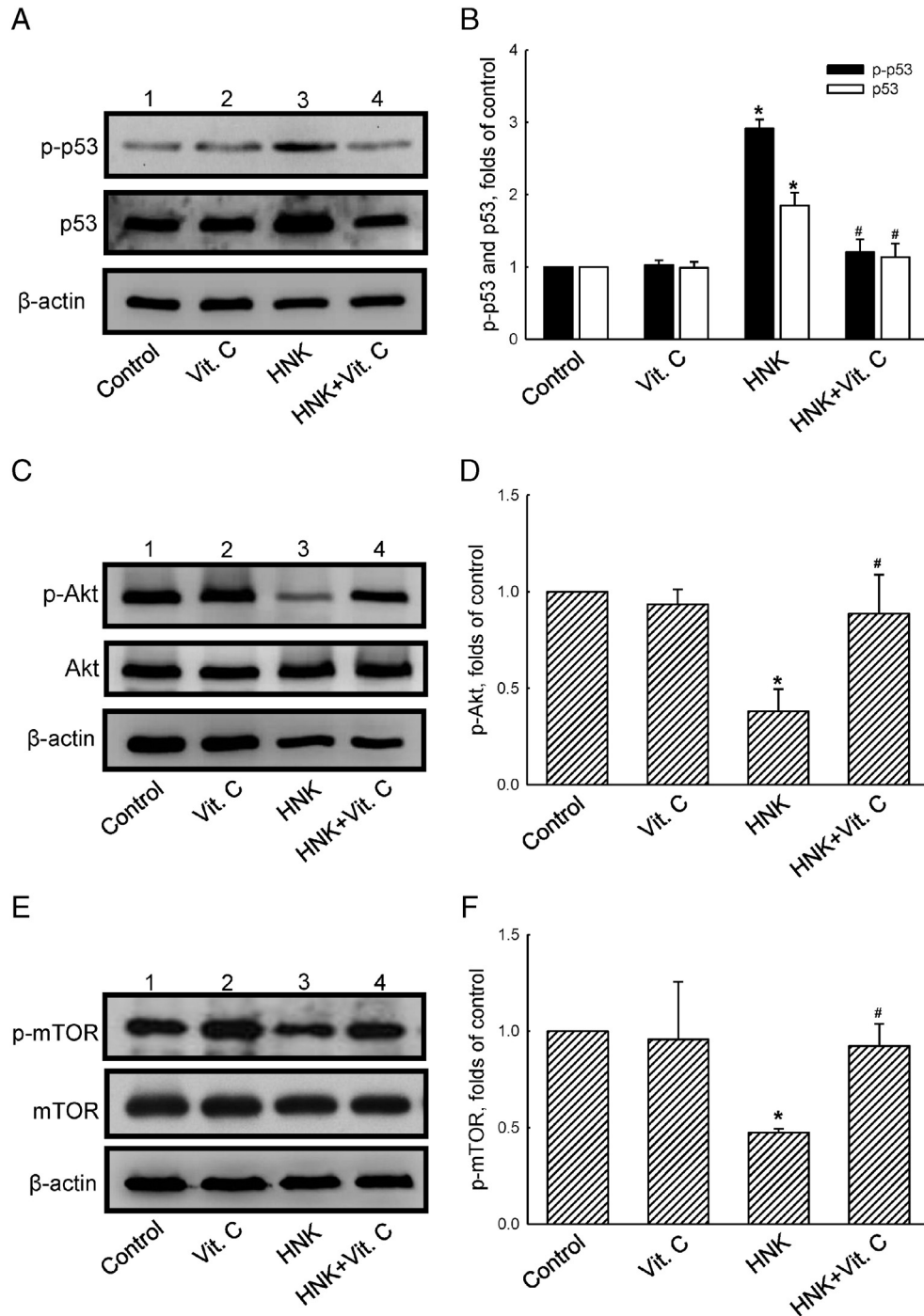


**Fig. 6.** Reactive oxygen species (ROS) participate in honokiol (HNK)-induced activation of the p53/Akt/mammalian target of rapamycin (mTOR) signaling pathway. Human glioma U87 MG cells were pretreated with 250  $\mu$ M vitamin C (Vit. C) for 1 h and then exposed to 40  $\mu$ M HNK for another 72 h. Levels of p-p53 and p53 were immunodetected (A, top two panels).  $\beta$ -Actin was detected as the internal control (bottom panel). These protein bands were quantified and statistically analyzed (B). Amounts of p-Akt and p-mTOR were analyzed (C and E, top panels). Akt, mTOR, and  $\beta$ -actin were detected as the internal controls (C and E, bottom panels). These protein bands were quantified and statistically analyzed (D and F). Each value represents the mean  $\pm$  SEM from three independent experiments. The symbols \* and # indicate that values significantly ( $p < 0.05$ ) differed from the respective control and honokiol-treated groups, respectively.

#### 4. Discussion

Previous studies, including ours, proved that honokiol has anticancer effects through inducing cell cycle arrest and apoptosis (Xu et al., 2011; Ishikawa et al., 2012; Lin et al., 2012a, 2012b). Our previous study also proved that honokiol can induce p53-mediated cell cycle arrest and apoptosis in human U87 MG glioma cells. In a continuation of those results, herein we revealed that honokiol can induce autophagy of glioma cells in vitro and in vivo. Exposure to honokiol induced LC3 protein expression in brain tumor sections from mice with an intracranial glioma, and caused LC3 processing in glioma cells and tumor tissues. Honokiol increased the percentage of autophagy of human glioma U87 MG cells in dose- and time-dependent manners. In addition, autophagic flux assays also proved the induction of autophagy in glioma cells (see Fig. 1 in Wu et al., 2016). In addition, honokiol could increase levels of beclin-1, an upstream marker of autophagy, in U87 MG cells (see Fig. 2 in Wu et al., 2016). Chang et al. (2013) showed the effects of honokiol on induction of autophagy in glioblastoma multiforme cells (Chang et al., 2013). Moreover, this study showed that suppression of autophagy consequently lowered apoptosis of human glioma cells. Therefore, honokiol can induce apoptosis and autophagic death of cancer cells.

Apoptosis and autophagy are classified as programmed cell death (Baehrecke, 2003). However, there is an interconnection between autophagy and apoptosis. Both may result in cell death and cooperate during this process (Jain et al., 2013). For example, autophagy was reported to result in traumatic brain injury-induced apoptosis (Lin et al., 2014). Our previous study showed that honokiol induced caspase-3 activation in a time-dependent manner (Lin et al., 2016). In this study, inhibition of autophagy by 3-MA decreased apoptosis and reversed cell viability; induction of autophagy by rapamycin further caused apoptosis of glioma cells. Our results suggest that honokiol-induced autophagy contributes to apoptotic cell death. On the contrary, pro-survival autophagy also occurred in some models to reduce apoptosis, such as imatinib-treated gastrointestinal stromal tumor cells and cisplatin-treated gastric cancer cells (Gupta et al., 2010; Zhang et al., 2013). Thus, the role of honokiol-induced autophagy in different cancer cells is still controversial.

Previous studies proved that the PI3K/Akt/mTOR signaling pathway is involved in autophagy induction (Jones, 2009; Zhang et al., 2013). Herein, after treating glioma cells with honokiol, autophagy was induced and was accompanied by reduced protein levels of PI3K, p-Akt, and p-mTOR at 24 h. Results of intracranial U87 MG glioma xenografts also showed that levels of p-Akt and p-mTOR were suppressed after administration of honokiol (see Fig. 3 in Wu et al., 2016). Similarly, honokiol causes autophagic cell death of B16-F10 melanoma cells partly through decreasing phosphorylation of Akt and mTOR (Gupta et al., 2010). Those studies concluded that the Akt/mTOR signaling pathway may be involved in honokiol-induced autophagy. Additionally, hypoxia has been shown to regulate autophagy of cancer cells (Patingre et al., 2008). Suzuki et al. (2013) reported that a combined treatment with celecoxib and  $\gamma$ -irradiation could synergistically induce autophagy of hypoxic glioblastoma cells. Thus, hypoxia may be another critical factor that can synergistically induce autophagy of glioma cells with honokiol.

In addition to cell cycle arrest, senescence, and apoptosis, p53 can stimulate autophagy (Chen and Karantzis-Wadsworth, 2009). Feng et al. proved that p53 inhibited mTOR activity by activating AMPK and subsequently activating the TSC1/TSC2 complex (Kaushik et al., 2012). Recently, honokiol was reported to activate Sirt3, an upstream protein of AMPK (Pillai et al., 2015; Lai et al., 2016). Activation of p53 results in upregulation of unc-51-like kinase 1/2, which is necessary for sustained autophagy in response to camptothecin-induced DNA damage (Feng et al., 2005). Moreover, induction of the damage-regulated autophagy modulator, a lysosomal protein, by p53 induces autophagy and results in cell death in cooperation with one or more other p53-dependent apoptotic signals (Crighton et al., 2006; Gao et al., 2011). Our previous study has verified the time-dependent activation of p53 by

honokiol (Lin et al., 2016). Herein, we demonstrated that p53 also contributes to autophagy induction. Chemical or genomic inhibition of p53 decreased autophagy and reversed the phosphorylation of Akt and mTOR in honokiol-treated U87 MG glioma cells, suggesting that honokiol induces autophagy through activating the p53-mediated Akt/mTOR signaling pathway. However, determining how p53 regulates mTOR after honokiol treatment requires further investigation.

Numerous studies have demonstrated that increased ROS stress in cancer cells leads to apoptosis (Kim et al., 2011; Wang et al., 2012; Huang et al., 2013). In wild type p53 melanoma cells, honokiol derivatives can also induce ROS (Fried and Arbiser, 2009; Bonner et al., 2016). However, other studies indicated that ROS participate in autophagy to regulate cell survival. A novel celecoxib derivative, OSU-03012, induced ROS-related autophagic cell death in hepatocellular carcinoma (Gao et al., 2008). Silibinin triggered ROS generation, including  $H_2O_2$  and  $O_2^{\bullet-}$ , to induce autophagic and apoptotic cell death of HT1080 human fibroblast cells (Duan et al., 2010). In this study, cytosolic  $H_2O_2$  was generated after treatment with honokiol at 0.5–48 h and was suppressed by vitamin C, resulting in a decrease in autophagic and apoptotic cell death of glioma cells. Our results showed that honokiol-induced autophagy contributes to glioma cell death through ROS generation. This study suggests that ROS may cause cell death via apoptosis and/or autophagy. However, the role of ROS-induced autophagy in cell death is still controversial.

ROS may act as both an upstream signal that triggers p53 activation and as a downstream mediator of p53-dependent apoptosis (Liu et al., 2008). DNA damage induced by ROS and chemotherapeutic agents promotes p53 activation, which causes caspase-dependent apoptosis and poly(ADP-ribose) polymerase-1-mediated necrosis (Montero et al., 2013). Isoorientin induced both apoptosis and autophagy by ROS-related p53, PI3K/Akt, JNK, and p38 signaling pathways in HepG2 cancer cells (Yuan et al., 2014). Similarly, our results showed that ROS accumulation by honokiol activated p53 in U87MG cells, thus consequently regulating the Akt/mTOR pathway which resulted in autophagy. However, physalin A induced apoptotic cell death via p53-mediated ROS generation, and induced protective autophagy against apoptosis in human melanoma A375-S2 cells (He et al., 2013). Those studies showed that interlinks between ROS and p53 are complex, and outcomes may be determined by various stimuli or cell types.

In conclusion, our results proved for the first time that treating U87 MG glioma cells with honokiol induced p53-mediated autophagic cell death possibly through downregulating PI3K/Akt/mTOR signaling. In addition, vitamin C, an antioxidant, improved cell survival by inhibiting autophagy and apoptosis, which indicates the important role of ROS in regulating honokiol-induced cell death. Therefore, this study showed a novel anticancer effect of honokiol, which supports its potential as a clinical therapeutic agent for brain tumors.

#### Transparency document

The transparency document associated with this article can be found, in the online version.

#### Acknowledgments

This study was supported by grants from the Health and Welfare Surcharge of Tobacco Products (MOHW104-TDU-B-212-124001 and MOHW105-TDU-B-212-134001), Taipei, Taiwan.

#### References

- Aoki, H., Takada, Y., Kondo, S., Sawaya, R., Aggarwal, B.B., Kondo, Y., 2007. Evidence that curcumin suppresses the growth of malignant gliomas in vitro and in vivo through induction of autophagy: role of Akt and extracellular signal-regulated kinase signaling pathways. *Mol. Pharmacol.* 72, 29–39.
- Baehrecke, E.H., 2003. Autophagic programmed cell death in *Drosophila*. *Cell Death Differ.* 10, 940–945.

- Bonner, M.Y., Karlsson, I., Rodolfo, M., Arnold, R.S., Vergani, E., Arbiser, J.L., 2016. Honokiol bis-dichloroacetate (honokiol DCA) demonstrates activity in vemurafenib-resistant melanoma in vivo. *Oncotarget* 7, 12857–12868.
- Chang, K.H., Yan, M.D., Yao, C.J., Lin, P.C., Lai, G.M., 2013. Honokiol-induced apoptosis and autophagy in glioblastoma multiforme cells. *Oncol. Lett.* 6, 1435–1438.
- Chen, N., Karantza-Wadsworth, V., 2009. Role and regulation of autophagy in cancer. *Biochim. Biophys. Acta* 1793, 1516–1523.
- Cheng, Y., Zhang, Y., Zhang, L., Ren, X., Huber-Keener, K.J., Liu, X., Zhou, L., Liao, J., Keihack, H., Yan, L., Rubin, E., Yang, J.M., 2012. MK-2206, a novel allosteric inhibitor of Akt, synergizes with gefitinib against malignant glioma via modulating both autophagy and apoptosis. *Mol. Cancer Ther.* 11, 154–164.
- Chilampalli, C., Guillermo, R., Kaushik, R.S., Young, A., Chandrasekher, G., Fahmy, H., Dwivedi, C., 2011. Honokiol, a chemopreventive agent against skin cancer, induces cell cycle arrest and apoptosis in human epidermoid A431 cells. *Exp. Biol. Med.* 236, 1351–1359.
- Codogno, P., Mehrpour, M., Proikas-Cezanne, T., 2011. Canonical and non-canonical autophagy: variations on a common theme of self-eating? *Nat. Rev. Mol. Cell Biol.* 13, 7–12.
- Crighon, D., Wilkinson, S., O'Prey, J., Syed, N., Smith, P., Harrison, P.R., Gasco, M., Garrone, O., Crook, T., Ryan, K.M., 2006. DRAM, a p53-induced modulator of autophagy, is critical for apoptosis. *Cell* 126, 121–134.
- Ding, W.X., Manley, S., Ni, H.M., 2011. The emerging role of autophagy in alcoholic liver disease. *Exp. Biol. Med.* 236, 546–556.
- Duan, W., Jin, X., Li, Q., Tashiro, S., Onodera, S., Ikejima, T., 2010. Silibinin induced autophagic and apoptotic cell death in HT1080 cells through a reactive oxygen species pathway. *J. Pharmacol. Sci.* 113, 48–56.
- Feng, Z., Zhang, H., Levine, A.J., Jin, S., 2005. The coordinate regulation of the p53 and mTOR pathways in cells. *Proc. Natl. Acad. Sci. U. S. A.* 102, 8204–8209.
- Fried, L.E., Arbiser, J.L., 2009. Honokiol, a multifunctional antiangiogenic and antitumor agent. *Antioxid. Redox Signal.* 11, 1139–1148.
- Gao, M., Yeh, P.Y., Lu, Y.S., Hsu, C.H., Chen, K.F., Lee, W.C., Feng, W.C., Chen, C.S., Kuo, M.L., Cheng, A.L., 2008. OSU-03012, a novel celecoxib derivative, induces reactive oxygen species-related autophagy in hepatocellular carcinoma. *Cancer Res.* 68, 9348–9357.
- Gao, W., Shen, Z., Shang, L., Wang, X., 2011. Upregulation of human autophagy-initiation kinase ULK1 by tumor suppressor p53 contributes to DNA-damage-induced cell death. *Cell Death Differ.* 18, 1598–1607.
- Gunther, W., Pawlak, E., Damasceno, R., Arnold, H., Terzis, A.J., 2003. Temozolomide induced apoptosis and senescence in glioma cells cultured as multicellular spheroids. *Br. J. Cancer* 88, 463–469.
- Gupta, A., Roy, S., Lazar, A.J., Wang, W.L., McAuliffe, J.C., Reynoso, D., McMahon, J., Taguchi, T., Floris, G., Debiec-Rychter, M., Schoffski, P., Trent, J.A., Debnath, J., Rubin, B.P., 2010. Autophagy inhibition and antimalarials promote cell death in gastrointestinal stromal tumor (GIST). *Proc. Natl. Acad. Sci. U. S. A.* 107, 14333–14338.
- Hay, N., Sonenberg, N., 2004. Upstream and downstream of mTOR. *Genes Dev.* 18, 1926–1945.
- He, H., Zang, L.H., Feng, Y.S., Chen, L.X., Kang, N., Tashiro, S., Onodera, S., Qiu, F., Ikejima, T., 2013. Physalin A induces apoptosis via p53-Noxa-mediated ROS generation, and autophagy plays a protective role against apoptosis through p38-NF- $\kappa$ B survival pathway in A375-S2 cells. *J. Ethnopharmacol.* 148, 544–555.
- Huang, A.C., Chang, C.L., Yu, C.S., Chen, P.Y., Yang, J.S., Ji, B.C., Lin, T.P., Chiu, C.F., Yeh, S.P., Huang, Y.P., Lien, J.C., Chung, J.G., 2013. Induction of apoptosis by curcumin in murine myelomonocytic leukemia WEHI-3 cells is mediated via endoplasmic reticulum stress and mitochondria-dependent pathways. *Environ. Toxicol.* 28, 255–266.
- Hwang, E.S., Park, K.K., 2010. Magnolol suppresses metastasis via inhibition of invasion, migration, and matrix metalloproteinase-2/-9 activities in PC-3 human prostate carcinoma cells. *Biosci. Biotechnol. Biochem.* 74, 961–967.
- Ishikawa, C., Arbiser, J.L., Mori, N., 2012. Honokiol induces cell cycle arrest and apoptosis via inhibition of survival signals in adult T-cell leukemia. *Biochim. Biophys. Acta* 1820, 879–887.
- Jain, M.V., Paczulla, A.M., Klonsch, T., Dimgba, F.N., Rao, S.B., Roberg, K., Schweizer, F., Lengerke, S., Davoodpour, P., Palicharla, V.R., Maddika, S., Łos, M., 2013. Interconnections between apoptotic, autophagic and necrotic pathways: implications for cancer therapy development. *J. Cell. Mol. Med.* 17, 12–29.
- Jones, R.G., 2009. The roles, mechanisms, and controversies of autophagy in mammalian biology. *Biol. Reprod.* 1, 68.
- Kanzawa, T., Bedwell, J., Kondo, Y., Kondo, S., Germano, I.M., 2003. Inhibition of DNA repair for sensitizing resistant glioma cells to temozolomide. *J. Neurosurg.* 99, 1047–1052.
- Kaushik, G., Ramalingam, S., Subramaniam, D., Rangarajan, P., Protti, P., Rammamoorthy, P., Anant, S., Mammen, J.M., 2012. Honokiol induces cytotoxic and cytostatic effects in malignant melanoma cancer cells. *Am. J. Surg.* 204, 868–873.
- Kim, E.H., Deng, C.X., Sporn, M.B., Liby, K.T., 2011. CDDO-imidazole induces DNA damage, G2/M arrest and apoptosis in BRCA1-mutated breast cancer cells. *Cancer Prev. Res.* 4, 425–434.
- Kondo, Y., Kanzawa, T., Sawaya, R., Kondo, S., 2010. The role of autophagy in cancer development and response to therapy. *Nat. Rev. Cancer* 5, 726–734.
- Lai, Y.C., Tabima, D.M., Dube, J.J., Hughan, K.S., Vanderpool, R.R., Goncharov, D.A., St Croix, C.M., Garcia-Ocaña, A., Goncharova, E.A., Tofovic, S.P., Mora, A.L., Gladwin, M.T., 2016. SIRT3-AMP-activated protein kinase activation by nitrite and metformin improves hyperglycemia and normalizes pulmonary hypertension associated with heart failure with preserved ejection fraction. *Circulation* 133, 717–731.
- Lin, J.W., Chen, J.T., Hong, C.Y., Lin, Y.L., Wang, K.T., Yao, C.J., Lai, G.M., Chen, R.M., 2012a. Honokiol traverses the blood-brain barrier and induces apoptosis of neuroblastoma cells via an intrinsic bax-mitochondrion-cytochrome c-caspase protease pathway. *Neuro-Oncology* 14, 302–314.
- Lin, C.J., Lee, C.C., Shih, Y.L., Lin, T.Y., Wang, S.H., Lin, Y.F., Shih, C.M., 2012b. Resveratrol enhances the therapeutic effect of temozolomide against malignant glioma in vitro and in vivo by inhibiting autophagy. *Free Radic. Biol. Med.* 52, 377–391.
- Lin, C.J., Chen, T.H., Yang, L.Y., Shih, C.M., 2014. Resveratrol protects astrocytes against traumatic brain injury through inhibiting apoptotic and autophagic cell death. *Cell Death Dis.* 5, e1147.
- Lin, C.J., Chang, Y.A., Lin, Y.L., Chio, C.C., Chen, R.M., 2016. Preclinical effects of honokiol on treating glioblastoma multiforme via G1 phase arrest and cell apoptosis. *Phytomedicine* 23, 517–527.
- Liu, B., Chen, Y., St Clair, D.K., 2008. ROS and p53: a versatile partnership. *Free Radic. Biol. Med.* 44, 1529–1535.
- Mehrpour, M., Esclatine, A., Beau, I., Codogno, P., 2010. Overview of macroautophagy regulation in mammalian cells. *Cell Res.* 20, 748–762.
- Montero, J., Dutta, C., van Bodegom, D., Weinstock, D., Letai, A., 2013. p53 regulates a non-apoptotic death induced by ROS. *Cell Death Differ.* 20, 1465–1474.
- Morselli, E., Galluzzi, L., Kepp, O., Criollo, A., Maiuri, M.C., Tavernarakis, N., Madeo, F., Kroemer, G., 2009. Autophagy mediates pharmacological lifespan extension by spermidine and resveratrol. *Aging* 1, 961–970.
- Nagalingsam, A., Arbiser, J.L., Bonner, M.Y., Saxena, N.K., Sharma, D., 2012. Honokiol activates AMP-activated protein kinase in breast cancer cells via an LKB1-dependent pathway and inhibits breast carcinogenesis. *Breast Cancer Res.* 14, R35.
- Pattingre, S., Espert, L., Biard-Piechaczyk, M., Codogno, P., 2008. Regulation of macroautophagy by mTOR and Beclin 1 complexes. *Biochimie* 90, 313–323.
- Pillai, V.B., Samant, S., Sundaresan, N.R., Raghuraman, H., Kim, G., Bonner, M.Y., Arbiser, J.L., Walker, D.L., Jones, D.P., Gius, D., Gupta, M.P., 2015. Honokiol blocks and reverses cardiac hypertrophy in mice by activating mitochondrial Sirt3. *Nat. Commun.* 6, 6656.
- Raha, S., Yumnam, S., Hong, G.E., Lee, H.J., Saralamma, V.V., Park, H.S., Heo, J.D., Lee, S.J., Kim, E.H., Kim, J.A., Kim, G.S., 2015. Naringin induces autophagy-mediated growth inhibition by downregulating the PI3K/Akt/mTOR cascade via activation of MAPK pathways in AGS cancer cells. *Int. J. Oncol.* 47, 1061–1069.
- Staudacher, I., Jehle, J., Staudacher, K., Pledl, H.W., Lemke, D., Schweizer, P.A., Becker, R., Katus, H.A., Thomas, D., 2014. HERG K<sup>+</sup> channel-dependent apoptosis and cell cycle arrest in human glioblastoma cells. *PLoS One* 9, e88164.
- Suzuki, K., Gerelchuluun, A., Hong, Z., Sun, L., Zenkoh, J., Moritake, T., Tsuboi, K., 2013. Celecoxib enhances radiosensitivity of hypoxic glioblastoma cells through endoplasmic reticulum stress. *Neuro-Oncology* 15, 1186–1199.
- Vousden, K.H., Lu, X., 2002. Live or let die: the cell's response to p53. *Nat. Rev. Cancer* 2, 594–604.
- Wang, Z.Y., Loo, T.Y., Shen, J.G., Wang, N., Wang, D.M., Yang, D.P., Mo, S.L., Guan, X.Y., Chen, J.P., 2012. LDH-A silencing suppresses breast cancer tumorigenicity through induction of oxidative stress mediated mitochondrial pathway apoptosis. *Breast Cancer Res. Treat.* 131, 791–800.
- Wang, Y., Zhu, X., Yang, Z., Zhao, X., 2013. Honokiol induces caspase-independent paraptosis via reactive oxygen species production that is accompanied by apoptosis in leukemia cells. *Biochem. Biophys. Res. Commun.* 430, 876–882.
- Wolf, I., O'Kelly, J., Wakimoto, N., Nguyen, A., Amblard, F., Karlan, B.Y., Arbiser, J.L., Koeffler, H.P., 2007. Honokiol, a natural biphenyl, inhibits in vitro and in vivo growth of breast cancer through induction of apoptosis and cell cycle arrest. *Int. J. Oncol.* 30, 1529–1537.
- Wu, G.J., Lin, C.J., Lin, Y.W., Chen, R.M., 2016. Analyses of honokiol-induced autophagy of human glioma cells *in vitro* and *in vivo*. *Data Brief* (submitted for publication).
- Xu, H.L., Tang, W., Du, G.H., Kokudo, N., 2011. Targeting apoptosis pathways in cancer with magnolol and honokiol, bioactive constituents of the bark of *Magnolia officinalis*. *Drug Discov. Ther.* 5, 202–210.
- Yoshimori, T., 2004. Autophagy: a regulated bulk degradation process inside cells. *Biochem. Biophys. Res. Commun.* 313, 453–458.
- Yuan, L., Wei, S., Wang, J., Liu, X., 2014. Isoorientin induces apoptosis and autophagy simultaneously by reactive oxygen species (ROS)-related p53, PI3K/Akt, JNK, and p38 signaling pathways in HepG2 cancer cells. *J. Agric. Food Chem.* 62, 5390–5400.
- Zhang, H.Q., He, B., Fang, N., Fang, N., Lu, S., Liao, Y.Q., Wan, Y.Y., 2013. Autophagy inhibition sensitizes cisplatin cytotoxicity in human gastric cancer cell line SGC7901. *Asian Pac. J. Cancer Prev.* 14, 4685–4688.
- Zhuang, W., Qin, Z., Liang, Z., 2009. The role of autophagy in sensitizing malignant glioma cells to radiation therapy. *Acta Biochim. Biophys. Sin.* 41, 341–351.